

Study of negative thermal expansion in the frustrated spinel ZnCr_2Se_4

X. L. Chen,¹ Z. R. Yang,^{1, a)} W. Tong,² Z. H. Huang,² L. Zhang,² S. L. Zhang,² W. H. Song,¹ L. Pi,^{2, 3} Y. P. Sun,^{1, 2} M. L. Tian,² and Y. H. Zhang^{2, 3}

¹⁾Key Laboratory of Materials Physics, Institute of Solid State Physics, Chinese Academy of Sciences, Hefei 230031, People's Republic of China

²⁾High Magnetic Field Laboratory, Chinese Academy of Sciences, Hefei 230031, People's Republic of China

³⁾University of Science and Technology of China, Hefei 230026, People's Republic of China

(Dated: 27 February 2022)

The origin of negative thermal expansion (NTE) in the bond frustrated ZnCr_2Se_4 has been explored. ESR and FTIR document an ideal paramagnetic state above 100 K, below which ferromagnetic clusters coexist with the paramagnetic state down to T_N . By fitting the inverse susceptibility above 100 K using a modified paramagnetic Curie-Weiss law, an exponentially changeable exchange integral J is deduced. In the case of the variable J , magnetic exchange and lattice elastic energy couple with each other effectively via magnetoelastic interaction in the ferromagnetic clusters, where NTE occurs at a loss of exchange energy while a gain of lattice elastic one.

I. INTRODUCTION

Magnetic frustrated systems have recently been a subject of continuing interests for a manifold of fascinating states such as spin ice, spin liquid and orbital glass *et al.* may be surviving down to $T = 0$.¹⁻³ Among the reported materials, chromium-based spinels with the formula ACr_2X_4 ($X = \text{O}, \text{S}, \text{Se}$) are of essential role not only of being theoretical interests but also in exploring potential multi-functional materials.⁴⁻⁷ For instance, in CdCr_2S_4 , the ferroelectricity and colossal magneto-capacitive coupling were observed.⁸ The compound was suggested to be a multiferroic relaxor. However, Scott and coworkers argued its correctness and rather related it to be a conductive artefact.⁹ Recently, the conclusion of conductive artefact is further evidenced by Yang *et al.*, both experimentally and theoretically.^{10,11} As a result, the design or tuning of multi-functional materials for potential applications enables the necessity to clear what stands behind the novel phenomena observed.

ZnCr_2Se_4 with negative thermal expansion (NTE) is a case in point.^{6,12} This compound exhibits a large positive Curie-Weiss temperature.¹³ However, neutron diffraction study revealed at $T_N = 21$ K a complex helical spins consisted of FM layers along [001] with a turning angle of 42° between the adjacent ones.¹⁴⁻¹⁶ Interestingly, this spin configuration allows a field-induced electric polarization revealing magnetoelectric effect or multiferroicity.^{17,18} While early X-ray diffraction (XRD) and neutron powder diffraction indicated a tetragonal structural transformation at T_N , subsequent neutron and synchrotron radiation results on single crystal showed an orthorhombic phase.^{15,16,19} Moreover, recent neutron powder diffraction found no sign of structural transition.¹² In fact, the exact lattice symmetry is still subject of debate. On the other hand, IR spectroscopy experiment reported a

marked splitting of the low-frequency mode below T_N .²⁰ This elucidates an essential spin-phonon coupling. Both geometrical and additional bond frustration are believed to be crucial factors.^{6,21} In addition, since Cr^{3+} in an octahedral crystal field is Jahn-Teller inactive, spin-phonon coupling is of vital importance in lifting frustration. Nevertheless, the very origin of NTE is yet far from being well understood.

In the present paper, a set of experimental techniques is utilized to probe the spin-lattice correlation in ZnCr_2Se_4 . By considering a variable exchange integral J with respect to temperature or lattice constant, NTE is attributed to a result of the competition between magnetic exchange and lattice elastic energy via magnetoelastic coupling.

II. EXPERIMENTS

The polycrystalline sample of ZnCr_2Se_4 was prepared by standard solid state reaction method. High purity powders of zinc (99.9%), chromium (99.9%) and selenium (99.9%) were mixed according to the stoichiometric ratio. Next, the powders were sealed in an evacuated quartz tube, and heated slowly to 850°C in seven days. Then the sample was reground, pelletized, sealed and heated again for another three days at 850°C . The magnetic data was collected on a Quantum Design superconducting quantum interference device (SQUID) magnetometer. The temperature dependent XRD patterns were obtained using XRD (Rigaku TTRIII). ESR measurements were performed using a Bruker EMX plus 10/12 CW-spectrometer at X-band frequencies ($\nu = 9.39$ GHz) in a continuous He gas-flow cryostat for 2–300 K. The transmittance spectra were collected in the far-infrared range using the Bruker Fourier-transform spectrometer Vertex 80v equipped with a He bath for 5–300 K.

^{a)}Corresponding author: zryang@issp.ac.cn

III. RESULTS AND DISCUSSION

The XRD data was analyzed using the standard Rietveld technique, which shows a single-phase material with cubic spinel structure at room temperature. Figure 1(a) shows the temperature (T) dependence of lattice constant a . With decreasing temperature, a first decreases rapidly and then manifests a negative thermal expansion behavior below about $T_E = 60$ K, which is almost concordant with the previous results.^{6,12} Upon further cooling below 20 K, splitting of several peaks in XRD spectra are observed. The representative peak (440) at 12 K that splits into (440) and (404) is presented in Fig. 1(b). This signals a cubic to tetragonal structural transition with space group $I4_1/amd$.^{15,19}

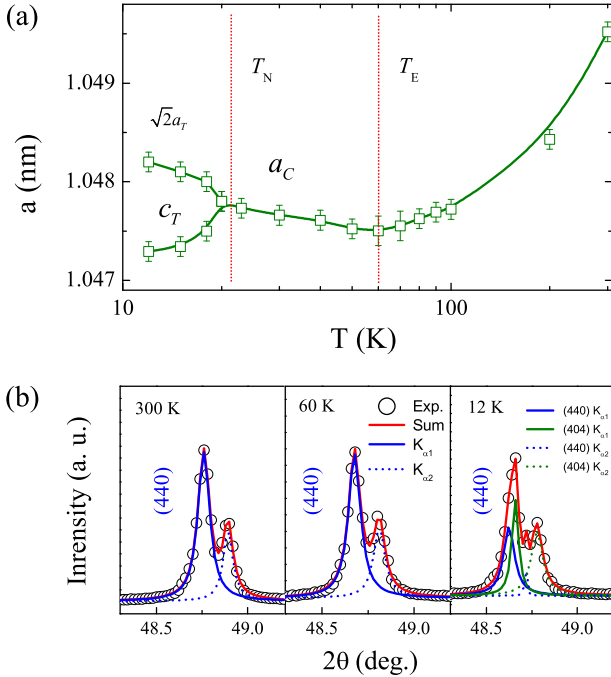


FIG. 1. (Color online) (a) Temperature dependent lattice parameter a vs T in semilogarithmic for ZnCr_2Se_4 . Error bars are average of repeated fittings. The negative thermal expansion initial temperature T_E and the antiferromagnetic order one T_N are drawn in red dotted lines. (b) The representative peaks (440) at 300 K, 60 K and 12 K. Circles are experimental data; Solid and dashed lines are Lorentzian fits.

Figure 2(a) presents the magnetization (M) versus T at low applied magnetic field of 100 Oe under both zero-field-cooled (ZFC) and field-cooled (FC) sequences. At about $T_N = 22$ K, M shows a sharp AFM transition.^{6,12,14–16} Figure 2(b) shows a fitting of the inverse susceptibility $1/\chi$ according to the paramagnetic (PM) Curie-Weiss law $\frac{1}{\chi} = \frac{T - \Theta_{CW0}}{C}$. A large positive Curie-Weiss temperature $\Theta_{CW0} = 85$ K and the coefficient $C = 3.74$ are obtained. The effective magnetic

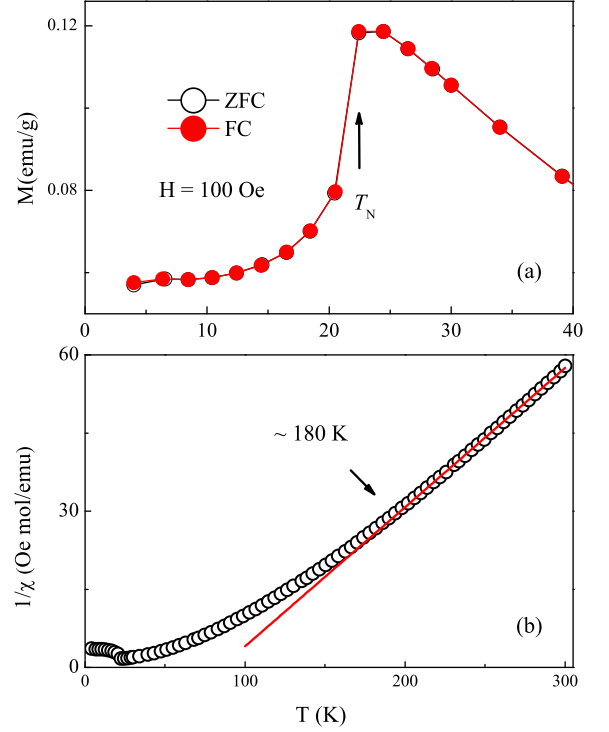


FIG. 2. (Color online) (a) Low temperature dependence of the magnetization M for a polycrystalline sample ZnCr_2Se_4 at 100 Oe. (b) A Curie-Weiss fitting of the inverse susceptibility.

moment calculated by the formula $\mu_{\text{eff}} = 2.83\sqrt{C/2}$ (in CGS units) equals to $3.87\mu_B$, in agreement with the spin-only Cr^{3+} ion.

The large positive Curie-Weiss temperature implies a dominant FM exchange interaction, however, the compound shows an AFM ordering at low temperatures. Hence, we first investigate the lattice dynamic inspired by the strong spin-lattice correlation. Within the wave-number range inspected, three infrared modes, labeled as *I*, *II* and *III* are observed simultaneously. Generally speaking, the phonon eigenfrequency follows an anharmonic behavior, which can be described by the following formula:

$$\omega_i = \omega_{0i} \left[1 - \frac{\alpha_i}{\exp(\Theta/T) - 1} \right], \quad (1)$$

where ω_{0i} , α_i and Θ are the eigenfrequency of mode i with decoupling of the spin and phonon at 0 K, the weight factor of mode i and the Debye temperature $\Theta = 309$ K.²⁰ A detailed temperature dependence of eigenfrequency is exhibited in Fig. 3. The solid line is a fitting of classical anharmonic behavior according to equation 1. Mode *I* shows negative shifts below T_E and Mode *II* shows positive shifts from about 100 K compared to the normal anharmonic behaviors, respectively. According to Lutz *et al.* and coworkers, the highest frequency mode *III* is ascribed to the Cr-Se vibration, however, modes *II*

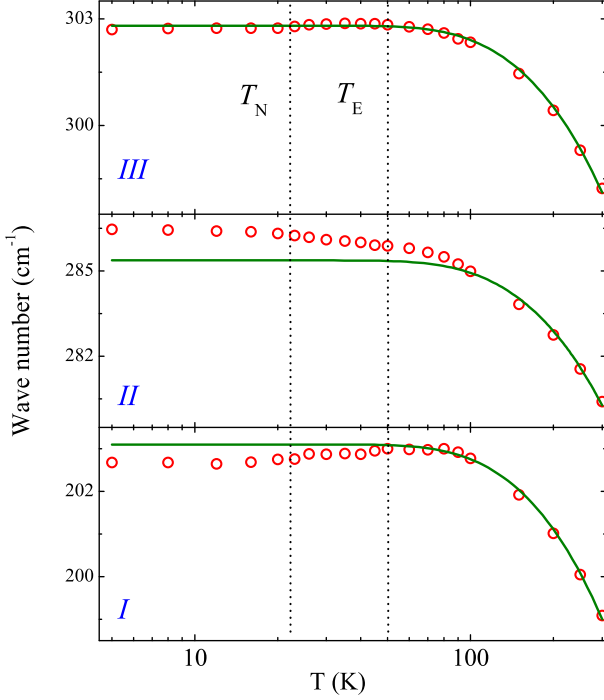


FIG. 3. (Color online) Temperature dependence of wave number of the infrared activated mode *I*, *II* and *III* for ZnCr_2Se_4 . The solid curve is a fit described in the text. The characteristic temperatures are indicated.

and *I* originate from combined vibrations of Cr-Se and Zn-Se. For mode *II*, the ratio of contribution from Cr-Se and Zn-Se is 78 : 18, while for mode *I* the ratio of Cr-Se to Zn-Se is 21 : 73.²² Cr-Se bond relates to the ferromagnetic (FM) spin super-exchange interaction and Zn-Se links to the antiferromagnetic (AFM) super-exchanges.⁴ As a result, FM Cr-X-Cr bonds dominate modes *II* and *III* while AFM linkages Cr-X-A-X-Cr determine mainly the eigenfrequency of mode *I*.^{23,24} The deviation of mode *II* below 100 K due to spin-phonon coupling indicates that FM fluctuations involve already at this temperature. Furthermore, the opposite shifts of modes *I* and *II* in the NTE temperature region may refer to a dynamic competition of FM and AFM superexchanges.

The temperature dependent ESR spectrum is further investigated. A PM signal is observed at room temperature and it vanishes below T_N (not drawn). The resonant field (H_{res}) and peak-to-peak line-width (ΔH_{PP}) as a function of temperature are plotted in Fig. 4(a) and (b), respectively. A typical ESR spectrum at 100 K and fitting using the first-order derivative symmetric Lorentzian function are presented in the inset of Fig. 4(a). As can be seen from Fig. 4(a), with decreasing temperature from 300 K to 100 K, H_{res} shows a constant value while ΔH_{PP} decreases almost linearly. Upon further cooling, H_{res} drops drastically and accordingly ΔH_{PP} broadens greatly, in accordance with Ref.⁶.

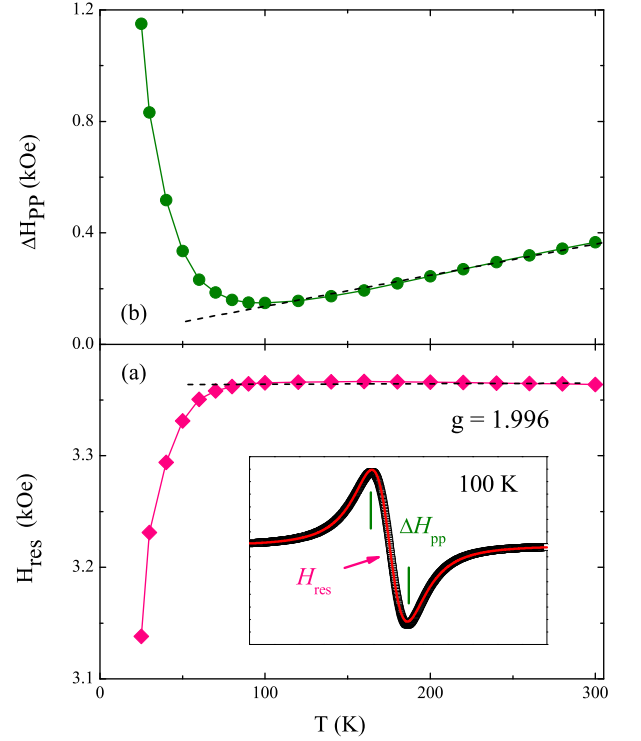


FIG. 4. (Color online) (a) Temperature dependence of the resonance field H_{res} . Inset: a typical fitting of the ESR spectrum at 100 K, where the definitions of the parameters are shown. (b) The peak-to-peak linewidth ΔH_{PP} vs T . The dashed lines are guided by eyes.

The g factor is 1.996, in agreement well with the previous works.^{6,25,26} The linear decrease of ΔH_{PP} with temperature can be attributed to a single-phonon spin-lattice relaxation mechanism.^{27,28} Both the constant g -factor and linear behavior of ΔH_{PP} evidence a well-defined paramagnetic (PM) state at least above 100 K. Note that H_{res} starts to decrease and ΔH_{PP} broadens at 100 K. Meanwhile, an FM-related positive shift for Mode *II* is observed in the IR modes in Fig. 3. These can thereby be correlated to the onset of FM fluctuations and spin-phonon coupling. As we know, H_{res} is a sum of H_{int} and H_{ext} , where H_{int} and H_{ext} are the equivalent internal and the external actual fields, respectively. For the case $H_{\text{int}} > 0$, the internal field may shift the resonance line to lower field; on the contrary, the resonance signal would appear at higher field with negative internal magnetic field. The decreasing of H_{res} below 100 K indicates an increasing of H_{int} , which may be caused by the interaction between the localized magnetic moments and the demagnetization effect.²⁷ Therefore, the enhancement of H_{int} and onset of FM fluctuations reveal gradually growing FM clusters, forming an FM-cluster and PM mixed state from 100 K to T_N . The existence of FM clusters is also supported by the following NTE analysis. Below T_N , the signal disappears due to the AFM ordering transition.

As is discussed above, the system keeps a pure PM state at least above 100 K, so the inverse susceptibility should be described by the PM Curie-Weiss law down to this temperature. However, it departs from the linear behavior at a temperature as high as about 180 K, see Fig. 2(b). Recalling the fitting process in Fig. 2(b), we have assumed a constant Curie-Weiss temperature Θ_{CW0} , i.e., a constant magnetic exchange interaction J . The behavior of IR modes below 100 K implies a competition of FM and AFM superexchange interactions. In addition, the nearest neighbor FM Cr-Se-Cr and other neighbor AFM Cr-Se-Zn-Se-Cr superexchange interactions depend strongly on the lattice constant.⁴ It means that the total J may change since a decreases dramatically upon cooling [Fig. 1(a)]. Accordingly, the traditional Curie-Weiss behavior should be modified within the present case to bridge the gap mentioned above. In specific, one should take a variable Θ_{CW} (or J) as a function of T or a into account.

In AFM spinel oxides, the Curie-Weiss temperature changes exponentially with the lattice parameter.²³ Naturally, an empirical description of $\Theta_{CW}(T) = \Theta_{CW0} - \alpha \times e^{-T/\beta}$ is postulated. The fitting of the inverse susceptibility above 100 K using the modified Curie-Weiss behavior $\frac{1}{\chi} = \frac{T - \Theta_{CW}(T)}{C}$ is exhibited in Fig. 5(a). The parameters are $\alpha = 226$ and $\beta = 45$. Furthermore, a remarkable deviation below 100 K in blue short dashed line indicates the appearance of the effective internal field originating from FM clusters. Next, based on the obtained α and β , $\Theta_{CW}(T)$ is extrapolated to low temperatures as exhibited in Fig. 5(b). It shows a derivation at about 180 K from the nearly constant value. With further lowering temperature, it decreases faster and faster and below $T \approx 45$ K, $\Theta_{CW}(T)$ even becomes negative. These features may interpret qualitatively the fact that ZnCr_2Se_4 is dominated by ferromagnetic exchange interaction but orders antiferromagnetically at low temperatures. Since the exchange integral and the Curie-Weiss temperature are linked by $J(T) \propto \Theta_{CW}(T)$ [$J(a) \propto \Theta_{CW}(a)$], we will use $J(T)$ [$J(a)$] instead in the following discussion.

Given that J is changeable, magnetic exchange and lattice elastic energies can link effectively with each other via magnetoelastic coupling. The free energy F in a magnetoelastic system is expressed as

$$F(T) = -J(T) \sum_{i,j} \vec{S}_i \cdot \vec{S}_j + \frac{1}{2} N \omega^2 \Delta^2(T) - T \cdot S(T), \quad (2)$$

where N the number of the ion sites, ω the averaged vibrational angular frequency and Δ the averaged strain relative to the equilibrium lattice constant. The first term is exchange energy (E_{ex}) as a function of J , the second is lattice elastic energy (E_{el}) related mainly to the lattice parameter a (or equivalent T) and the last is the entropy. From the above equation we know that if the system stays at an ideal PM state, then $E_{ex} = 0$. So E_{ex} and E_{el} will show no coupling, as is observed from the IR spectra above 100 K.

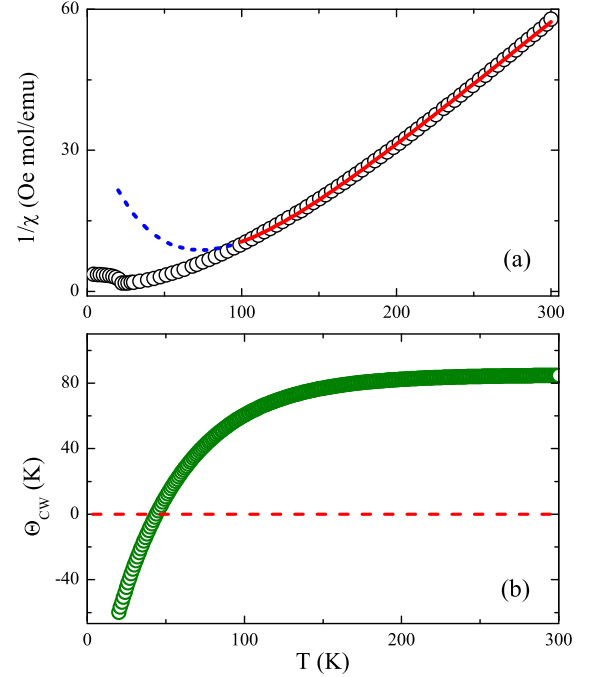


FIG. 5. (Color online) (a) A fitting of the inverse susceptibility above 100 K in red solid line using $\frac{1}{\chi} = \frac{T - \Theta_{CW}(T)}{C}$ taking a temperature or lattice constant a dependent Curie-Weiss temperature into account. The short dashed blue line is an extension of the fitting to low temperatures. (b) Θ_{CW} vs T and the red dashed line indicates $\Theta_{CW} = 0$ at 45 K.

When the system stays at an FM state with a changeable J , there may exist a competition between E_{ex} and E_{el} since the former is negative while the latter always positive. Indeed, it has been concluded above that J decreases exponentially [Fig. 5(a)] and some FM clusters forms gradually below 100 K. Therefore, the concomitant decrease of J and a causes an increasing E_{ex} but decreasing E_{el} in the FM clusters. At some critical point, a totally compensation between them may present. If a further decreases as cooling, the variation of E_{ex} would gradually exceed that of E_{el} in magnitude. Especially when J drops sharply with respect to a , say here at T_E , a tiny decrement of a will give rise to a dramatic increment of E_{ex} whereas E_{el} keeps nearly constant. The state in a system subjected to stimuli, such as cooling, always tends to develop towards one that can lower F . In this sense it is favorable to lowering F by expanding the lattice parameter a to increase J ($J > 0$) and thereby to decrease E_{ex} due to its negative value, at the same time at a cost of few increases of E_{el} in magnitude. This means that a negative thermal expansion of the lattice originating from the FM clusters with a exponentially changeable J is expected. It is worthy of noting that when applying a magnetic field to the system in the NTE temperature region, NTE in magnitude enhances.⁶ This is because the size or population of the FM clusters

increases when applying a magnetic field.

On the contrary, when an AFM ordering appears, J becomes negative and the condition to stimulate NTE is not met any more. Normal thermal expansion upon cooling results in a simultaneous decreasing of E_{ex} and E_{el} , which is consistent to lowering F . In fact, a normal expansion feature is observed below T_N .⁶ It should be noted that the existence of NTE^{6,12} evidences in turn that J is changeable. If J keeps constant in a FM cluster, E_{ex} will be almost constant and a normal thermal expansion of the lattice alone can give rise to a decrease of E_{el} and of F sufficiently.

IV. CONCLUSIONS

To summarize, we have investigated the origin of NTE in strongly bond frustrated ZnCr_2Se_4 . By fitting the inverse susceptibility above 100 K, an exponentially variable exchange J is deduced. The exchange and lattice elastic energy can effectively couple with each other via magnetoelastic on basis of this changeable J . NTE is qualitatively interpreted as a competition between the two kinds of energy.

ACKNOWLEDGMENTS

This research was financially supported by the National Key Basic Research of China Grant, Nos. 2010CB923403, and 2011CBA00111, and the National Nature Science Foundation of China Grant 11074258.

¹J. S. Gardner, M. J. P. Gingras, and J. E. Greedan, *Rev. Mod. Phys.* **82**, 53 (2010).

²L. Balents, *Nature* **464**, 199 (2010).

³R. Tong, Z. R. Yang, C. Shen, X. B. Zhu, Y. P. Sun, L. Li, S. L. Zhang, L. Pi, Z. Qu, and Y. H. Zhang, *EPL* **89**, 57002 (2010).

⁴P. K. Baltzer, P. J. Wojtowicz, M. Robbins, and E. Lopatin, *Phys. Rev.* **151**, 367(1966).

⁵L. Q. Yan, J. Shen, Y. X. Li, F. W. Wang, Z. W. Jiang, F. X. Hu, J. R. Sun, and B. G. Shen, *Appl. Phys. Lett.* **90**, 262502 (2007).

⁶J. Hemberger, H.-A. Krug von Nidda, V. Tsurkan, and A. Loidl, *Phys. Rev. Lett.* **98**, 147203 (2007).

⁷I. Kim, Y. S. Oh, Y. Liu, S. H. Chun, J.-S. Lee, K.-T. Ko, J.-H. Park, J.-H. Chung, and K. H. Kim, *Appl. Phys. Lett.* **94**, 042505 (2009).

⁸J. Hemberger, P. Lunkenheimer, R. Fichtl, H.-A. Krug von Nidda, V. Tsurkan, and A. Loidl, *Nature* **434**, 364 (2005).

⁹G. Catalan, and J. F. Scott, *Nature* **448**, E4 (2007).

¹⁰Y. M. Xie, Z. R. Yang, L. Li, L. H. Yin, X. B. Hu, Y. L. Huang, H. B. Jian, W. H. Song, Y. P. Sun, S. Q. Zhou, and Y. H. Zhang, *J. Appl. Phys.* **112**, 123912 (2012).

¹¹Y. M. Xie, Z. R. Yang, Z. T. Zhang, L. H. Yin, X. L. Chen, W. H. Song, Y. P. Sun, S. Q. Zhou, W. Tong, and Y. H. Zhang, *EPL* **104**, 17005 (2013).

¹²F. Yokaichiya, A. Krimmel, V. Tsurkan, I. Margiolaki, P. Thompson, H. N. Bordallo, A. Buchsteiner, N. Stüßer, D. N. Argyriou, and A. Loidl, *Phys. Rev. B* **79**, 064423 (2009).

¹³F. K. Lotgering, *Proceedings of the International Conference on Magnetism, Nottingham, 1964* (Institute of Physics and the Physical Society, London, 1965), p. 533.

¹⁴R. Plumier, *J. Phys. (Paris)* **27**, 213 (1966).

¹⁵J. Akimitsu, K. Siratori, G. Shirane, M. Iizumi, and T. Watanabe, *J. Phys. Soc. Jpn.* **44**, 172 (1978).

¹⁶M. Hidaka, N. Tokiwa, M. Fujii, S. Watanabe, and J. Akimitsu, *Phys. Stat. Sol. B* **236**, 9 (2003).

¹⁷K. Siratori, and E. Kita, *J. Phys. Soc. Jpn.* **48**, 1443 (1980).

¹⁸H. Murakawa, Y. Onose, K. Ohgushi, S. Ishiwata, and Y. Tokura, *J. Phys. Soc. Jpn.* **77**, 043709 (2008).

¹⁹R. Kleinberger, and R. de Kouchkovsky, *C.R. Acad. Sci. Paris, Ser. B* **262**, 628 (1966).

²⁰T. Rudolf, Ch. Kant, F. Mayr, J. Hemberger, V. Tsurkan, and A. Loidl, *Phys. Rev. B* **75**, 052410 (2007).

²¹S.-H. Lee, C. Broholm, W. Ratcliff, G. Gasparovic, Q. Huang, T. H. Kim, and S. W. Cheong, *Nature (London)* **418**, 856 (2002).

²²J. Zwinscher, and H. D. Lutz, *J. Alloy Comp.* **219**, 103 (1988).

²³T. Rudolf, Ch. Kant, F. Mayr, J. Hemberger, V. Tsurkan, and A. Loidl, *New J. Phys.* **9**, 76 (2007).

²⁴K. Wakamura, and T. Arai, *J. Appl. Phys.* **63**, 5824 (1988).

²⁵J. J. Stickler, and H. J. Zeiger, *J. Appl. Phys.* **39**, 1021 (1968).

²⁶K. Siratori, *J. Phys. Soc. Jpn.* **30**, 709 (1971).

²⁷C. Rettori, D. Rao, J. Singley, D. Kidwell, S. B. Oseroff, M. T. Causa, J. J. Neumeier, K. J. McClellan, S.-W. Cheong, and S. Schultz, *Phys. Rev. B* **55**, 3083 (1997).

²⁸D. L. Huber, and M. S. Seehra, *J. Phys. Chem. Solids* **36**, 723 (1975).